Interaction of Alamethicin with Ether-Linked Phospholipid Bilayers: Oriented Circular Dichroism, ^{31}P Solid-State NMR, and Differential Scanning Calorimetry Studies

Paresh C. Dave, Emma Billington, Yeang-Ling Pan, and Suzana K. Straus
Department of Chemistry, University of British Columbia, Vancouver, British Columbia V6T 1Z1, Canada

ABSTRACT The arrangement of the antimicrobial peptide alamethicin was studied by oriented circular dichroism, ^{31}P solid-state NMR, and differential scanning calorimetry in ether-linked phospholipid bilayers composed of 1,2-O-dihexadecyl-*sn*-glycero-3-phosphocholine (DHPC). The measurements were performed as a function of alamethicin concentration relative to the lipid concentration, and results were compared to those reported in the literature for ester-linked phospholipid bilayers. At ambient temperature, alamethicin incorporates into the hydrophobic core of DHPC bilayers but results in more lipid disorder than observed for ester-linked 1-palmitoyl, 2-oleoyl-*sn*-glycero-3-phosphatidylcholine (POPC) lipid bilayers. This orientational disorder appears to depend on lipid properties such as bilayer thickness. Moreover, the results suggest that alamethicin inserts into the hydrophobic core of the bilayers (at high peptide concentration) for both ether- and ester-linked lipids but using a different mechanism, namely toroidal for DHPC and barrel-stave for POPC.

INTRODUCTION

Alamethicin is a well-characterized member of the peptaibol family, a class of short, antimicrobial peptides known to cause permeabilization of bacterial membranes. Peptaibols are generally α-helical in structure and form ion channels in microbial cell membranes in response to changes in transmembrane potential (reviewed in Jen et al. (1) and Bechinger (2,3)). Experimentally, they are found to be capable of forming transmembrane pores in the absence of a potential difference. This phenomenon requires certain structural and physiochemical conditions, several of which are not yet well defined (4–6). Alamethicin, like other membrane-active peptides, may assume one of two orientations when associated with lipid bilayers. In one arrangement, the peptide is adsorbed on the bilayer surface (3,4,7,8). In this case, the peptaibol is said to be in the inactive surface (*S*) state, and no active transmembrane pores can be detected by neutron diffraction (9). Under certain sample conditions, however, all the peptide molecules can adopt a transmembrane orientation, which is characteristic of the inserted (*I*) state (10), for which functional ion channels have been observed (4).

The insertion of alamethicin (and other antimicrobial peptides) into the membrane depends upon several factors, such as peptide/lipid (P/L) molar ratio, elasticity and structure of the bilayer, and physiological factors (e.g., degree of hydration) of the bilayer. In the case of the concentration (P/L), alamethicin has been specifically found to have a sigmoidal concentration dependence (6). That is, at very low P/L molar ratios, the *S* state is observed. However, above some critical threshold peptide concentration (P/L*) insertion of a fraction of the molecules occurs, and some lytic activity is detected (11,2). As the P/L ratio is increased, a coexistence region between the *S* and *I* states is observed, until the *I* state is eventually reached at very high P/L (7,10,13). It is worth noting that cytolytic activity may also be induced experimentally in the *S* state by applying a transmembrane voltage rather than increasing the P/L ratio (14). Much of this previous work has focused on determining the threshold P/L* value for alamethicin in various types of membranes under different physiological conditions to better explain the specificity of antimicrobial peptides for selected microbes (6,7,15,16). All these studies have been carried out using ester-linked phospholipid bilayers.

The aim of this study is to extend this work to lipid bilayers which have different properties (e.g., phase, bilayer thickness), namely ether-linked lipids. More specifically, we have chosen to investigate the concentration dependence of alamethicin in the ether-linker lipid di-hexadecyl phosphocholine (DHPC), which exists in an interdigitated phase at ambient temperature in the absence of any inducer (17–19). Such interdigitated bilayer structures have attracted considerable interest because of the different bilayer structures they can form and their possible implications for membrane function. In addition, ether-linked phospholipids have recently attracted much attention as a platelet-activating factor (20). They have also displayed antitumor activity and have been found to be the major lipid of archaebacterial membranes (21). From an NMR point of view, these types of lipids are also of interest as they do not possess any carbonyl moieties, which can be advantageous when studying membrane-interacting peptides, since the signal in the 180–170 ppm region of a ^{13}C spectrum would then arise solely from

Submitted May 30, 2005, and accepted for publication July 18, 2005.

Paresh C. Dave and Emma Billington contributed equally to this work.

Address reprint requests to Suzana K. Straus, Tel.: 604-822-2537; Fax: 604-822-2157; E-mail: sstraus@chem.ubc.ca.

0006-3495/05/10/2434/09 $2.00

doi: 10.1529/biophysj.105.067678

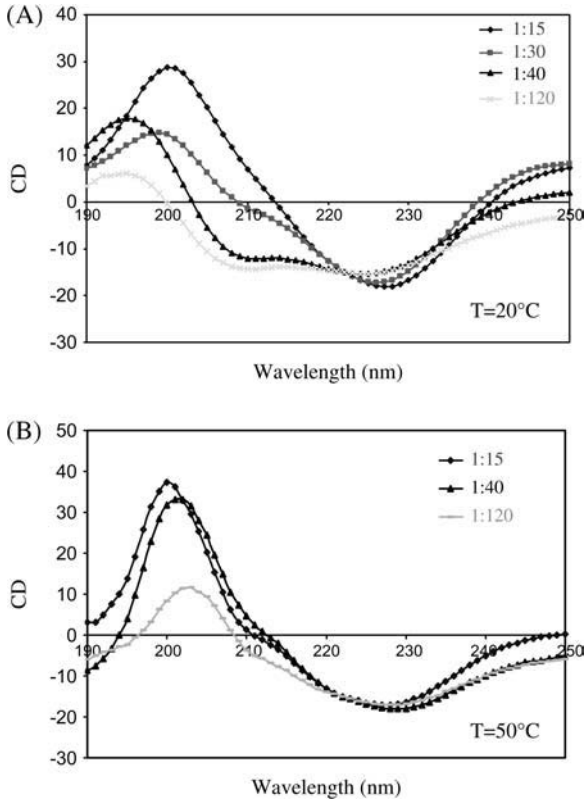

FIGURE 1 Overlay of OCD spectra of alamethicin at (*A*) 20°C in the presence of ether-linked DHPC as a function of peptide/lipid concentration: P/L = 1:15 (*diamonds*), P/L = 1:30 (*squares*), P/L = 1:40 (*triangles*), and P/L = 1:120 (*crosses*); and (*B*) at 50°C as a function of peptide/lipid concentration: P/L = 1:15 (*diamonds*), P/L = 1:40 (*triangles*), and P/L = 1:120 (*bars*).

the peptide (22,23). Finally, ether-linked lipids can be used to form bicelles (24–26).

To characterize the state (*I* or *S*) of alamethicin in DHPC, a combination of oriented circular dichroism (OCD), ^{31}P solid-state NMR, and differential scanning calorimetry (DSC) data were collected and analyzed. Each of these methods has been used to characterize the interaction of membrane-bound peptides with lipids in complementary ways. OCD spectroscopy can be applied to helical peptides bound to oriented planar phospholipid bilayers and thereby provide a direct measure of the orientational distribution of helices with respect to the incident light beam (7). The technique has proven particularly useful for tracking changes in alamethicin orientation which can occur in response to changes in peptide surface density, bilayer hydration, acyl-chain saturation, or lipid phase (4,5,7,27). ^{31}P solid-state NMR can be used to probe the degree alignment of lipid bilayers and the mobility of lipid headgroups, by using mechanically aligned phospholipid bilayers on glass plates (28–30). Using ^{31}P and ^{15}N NMR, for instance, Bechinger et al. (28) demonstrated how the insertion of alamethicin and the related peptaibol, zervamicin, depends on the hydrophobic thickness of the lipid bilayer relative to the peptide length. Finally, DSC is a powerful thermodynamic technique for probing the nature and stoichiometry of lipid-peptide interactions and for providing information about the location and aggregation state of peptides and their lipid-bound state (31). It has been used to probe phase transitions of pure phospholipids (32,33) and perturbations induced by lipid-interacting peptides (34–36). For instance, DSC studies carried out for multilamellar vesicle (MLV) samples composed of phospholipids isolated from *Thermoplasma acidophilum* and alamethicin have shown that the peptide broadens the lipid phase transition of the main phospholipid from *T. acidophilum* (37). Moreover, alamethicin was found to interact primarily with the lipid headgroups and to readily incorporate into the tetraether lipid structures.

Results from these three types of experiments applied to alamethicin in DHPC allow us to propose a mode of insertion of this peptaibol in an interdigitated ether-linked phospholipid for the first time. Comparison to the insertion of alamethicin in ester-linked membrane bilayers, in gel (1,2-dipalmitoyl-*sn*-glycero-3-phosphatidylcholine (DPPC)) or the Lα phase (1-palmitoyl, 2-oleoyl-*sn*-glycero-3-phosphatidylcholine (POPC)) at room temperature, is also made.

MATERIALS AND METHODS

Materials

DHPC, POPC, 1,2-diphytanoyl-*sn*-glycero-3-phosphatidylcholine (DPhPC), and DPPC were purchased from Avanti Polar Lipids (Alabaster, AL). POPC, DPhPC, and DHPC were obtained in chloroform, and DPPC was obtained in powder form. Alamethicin was purchased from Sigma-Aldrich Chemical (St. Louis, MO). Both peptide and lipid were used without further purification. Alamethicin was dissolved in a 1:1 v/v methanol/chloroform mixture to make a 0.125 μM stock solution.

Mechanically oriented sample preparation

For circular dichroism spectra, 0.5 μmol alamethicin (4 μL of stock solution) was mixed with the appropriate quantity of DPhPC, DHPC, or DPPC, already fully dissolved in 1:1 methanol/chloroform, in a 25 mL round bottom flask. The contents of the flask were sonicated for 10 min, and the resulting solution was dried under a stream of N_2 to produce a clear layer which coated the bottom of the flask. The sample was then vacuum dessicated overnight at room temperature to ensure that any residual solvent was removed. After drying, the sample was hydrated with 2 ml deionized water to yield a peptide concentration of 0.25 mM and sonicated until all lipid and peptide were fully dissolved. To prepare solution samples at a 1:30 P/L molar ratio, an 8× dilution was made of the appropriate hydrated solution. The diluted solution was used to measure solution circular dichroism in a clean quartz cuvette with 1.0 mm path length (*d*). To prepare oriented samples, 90 μL of the hydrated sample was deposited onto a clean quartz slide (the quartz slides had been thoroughly cleaned with both water and ethanol and allowed to air dry repeatedly) which measured 3 × 1 cm with thickness of 1 mm. Each slide was fitted with a spacer of thickness ~1 mm which formed a ~2 mm-wide frame around the slide. Spacers were made of six layers of stacked parafilm. The hydrated sample was deposited on each slide in small droplets via a syringe, ensuring that the mixture covered the entire surface area of the slide. This method resulted in the formation of oriented multilayers (38). Slides were then incubated overnight in a sealed dessicator at 93% relative humidity and 37°C. When removed

from the incubator, the hydrated sample was present on the slide as a clear gel-like layer. A clean second, dry quartz slide was placed on top of the parafilm spacer on the first slide and pressed firmly against it. For the NMR experiments, samples were prepared using the same procedure as described above, except that the sample was spread onto 20 glass slides (11 × 11 mm) and 1–3 mg of alamethicin was used.

Unoriented sample preparation

An aliquot corresponding to 25 mg of the appropriate lipid dissolved in chloroform was deposited into a test tube, along with the alamethicin. The chloroform was then removed using N_2 gas for 15–20 min. The test tube was placed in a vacuum dessicator overnight to remove any residual solvents. The lipid mixture was resuspended in 100 μL water by heating in a water bath at 50°C. Once all the phospholipids were fully dissolved, the MLV sample was transferred to an NMR rotor. For the $T1$ measurements, the samples were prepared using 50% (w/w) lipid, 50 mM TRIS buffer, pH 7.4, to which 1 mM EDTA was added, as outlined in Tamm and Seelig (39).

OCD spectroscopy

Circular dichroism measurements were made on a Jasco (Easton, MD) J-810 Spectrometer at 20°C and 50°C. At the latter temperature, samples were equilibrated for a minimum of 20–30 min before data acquisition. The spectra were acquired over a wavelength range of 250–190 nm, using 0.5 nm steps and a scan speed of 100 nm/min. To obtain an increased signal/noise ratio, each recorded spectrum was the average of three scans. Measurements were made with the incident light normal to the substrate surface (7). The light passed through a circular chasm 1 cm in diameter before reaching the quartz slide. The acquired spectrum did not change after lengthwise rotation of the quartz slide by 180°, indicating that neither spectral artifacts in the quartz nor inhomogeneities in the sample were contributing significantly to the spectra. Any contribution of the lipids to each spectrum was corrected for by subtracting a background spectrum, containing only lipid, from the spectrum obtained for the peptide-containing sample.

NMR spectroscopy

^{31}P NMR spectra were recorded on a Varian (Palo Alto, CA) 400-MHz NMR spectrometer operating at 161.80 MHz using a static double resonance flat coil (11 × 11 mm) probe for mechanically aligned bilayer samples and a Varian triple resonance TXI MAS probe equipped with a 4 mm diameter rotor for the MLV samples. The ^{31}P NMR spectra were recorded with ^{1}H decoupling using a 4.2 μs $\pi/2$ pulse and a 3 s recycle delay. For the ^{31}P NMR spectra, 1024 scans were taken and the free induction decay was processed using 100 Hz of line broadening. The spectral width was set to 50 kHz. The spectra for the aligned samples were repeated three times (i.e., using three different samples) for each P/L ratio to ensure that the spectra were reproducible.

Phosphorus $T1$ measurements were performed using an inversion-recovery pulse sequence π-τ-$\pi/2$ with proton decoupling and with a recycle time of 3 s (40,41) (see Supplemental Material for spectra). To first approximation, the inversion recovery of the whole powder pattern could be described by a single $T1$ value. Consequently, the $T1$ values were determined at the chemical shift value of −16 ppm for the MLV samples.

Differential scanning calorimetry

MLVs of DHPC, DPPC, DPhPC, 1:15 alamethicin/DHPC, and 1:80 alamethicin/DHPC, with a final lipid concentration of 25 mg/ml were prepared by dissolving the desired lipid in chloroform. The lipid samples were then dried under a stream of nitrogen and then further dried under vacuum overnight to remove any residual solvent. Alamethicin was added to the dried lipid sample at the desired P/L molar ratio. The samples were then resuspended with a buffer containing 20 mM HEPES pH 7.0 and 100 mM NaCl. The resuspended samples were vortexed vigorously three times while heating the sample above the phase transition peak (44°C–45°C) for 5 min in between each vortex step. The buffers and lipid samples were degassed for 5 min before loading the sample into a MC (multicell)-DSC (Calorimetry Sciences, South Provo, UT), located at the University of British Columbia Centre for Biological Calorimetry. The samples were heated and cooled between a temperature range of 5°C–90°C at a heating (cooling) rate of 0.333°C/min. The resulting data were converted to molar heat capacity and baseline corrected by subtracting a blank buffer scan. Each experiment was repeated at least twice to ensure reproducibility of the results.

RESULTS AND DISCUSSION

Fig. 1, *A* and *B*, shows the normalized (at the isodichroic point) OCD spectra of samples of fully hydrated alamethicin in ether-linked DHPC for a series of P/L ratios at 20°C and 50°C, respectively. At the lower temperature (i.e., below the transition temperature of DHPC), the OCD spectrum of alamethicin incorporated into the DHPC lipid bilayer, with a P/L ratio of 1:15, demonstrates a helix oriented parallel to the light or to the bilayer normal (*I* state), as described by Huang et al. (7,42). The OCD spectrum of sample containing P/L ratio 1:120 represents the helix oriented perpendicular to the light or to the bilayer normal (*S* state). These data suggest that the threshold peptide concentration (P/L*) for alamethicin/DHPC is between 1:40 and 1:30 at 20°C. Above the transition temperature for DHPC, i.e., at 50°C when DHPC is in liquid crystalline phase, the threshold P/L* ratio appears to no longer exist, indicating that alamethicin is inserted into the bilayer even at low concentrations, as is the case for alamethicin in POPC at room temperature as evidenced from ^{15}N NMR data (28). In Fig. 3, OCD spectra are shown of alamethicin incorporated in the ester-linked phospholipid DPPC at various lipid/peptide concentrations at 20°C (gel phase). It clearly indicates that for samples with P/L > 1:80, the helix is predominantly in the *I* state. OCD experiments were also performed for alamethicin incorporated into the ester-linked DPhPC, yielding identical results to those reported in the literature (16) (data not shown).

Figs. 1 and 2 therefore reveal that the threshold peptide concentration, P/L*, for DHPC is higher (between 1:40 and 1:30) than for alamethicin in DPPC (~1:80) at 20°C. This difference can be attributed to the different properties of these lipids. More specifically, recent experiments have shown that membrane thinning is the cause for sudden insertion of alamethicin in the lipid bilayer above the critical P/L* (7,11–13). Previous reports clearly indicate that the lipid composition, hydrophobic length, hydration, and ratio between the area of the headgroup region (A_{hg}) and the area of hydrocarbon chain region (A_{ch}), influence the membrane thinning process. In this study, the difference between the P/L threshold concentrations (P/L*) for DHPC and DPPC could be the result of several factors, such as the presence of different phases, the hydrophobic length difference, and/or

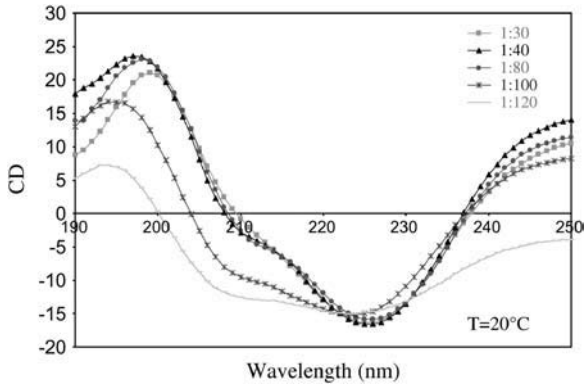

FIGURE 2 Overlay of OCD spectra of alamethicin in the presence of ester-linked DPPC as a function of peptide/lipid concentration, at room temperature: P/L = 1:30 (*squares*), P/L = 1:40 (*triangles*), P/L = 1:80 (*solid circles*), P/L = 1:100 (x), and P/L = 1:120 (*bars*).

differences in A_{hg}/A_{ch}. As hydration was carefully controlled during sample preparation, we assume that this would play a minor role in explaining the differences in P/L*.

As reported earlier, DHPC lipid bilayers are in interdigitated phase at room temperature (~22°C–24°C), whereas DPPC lipid bilayers are in gel phase. The hydrophobic length of alamethicin is 22 Å, whereas the distance between the phosphate groups, $d_{p\text{-}p}$, is 42 Å for DPPC bilayers and 31 Å for DHPC bilayers, at room temperature (43,44). Since a $d_{p\text{-}p}$ of 42 Å for DPPC implies that the hydrophobic thickness of the bilayer is 24 Å, the length of alamethicin and that of the DPPC bilayer are well matched. This has as a consequence that alamethicin would be better able to insert into DPPC than DHPC. Alternatively, the different areas occupied by the lipid headgroups and carbon chains may also play a role. Headgroup size of the phospholipids which constitute the bilayer often has a pronounced effect on the threshold P/L* of antimicrobial peptides, but in these OCD experiments for DHPC and DPPC, the phosphocholine headgroup region is similar. A comparison of the areal ratio between the headgroup and the hydrocarbon chains, A_{hg}/A_{ch} (45), however, shows that DHPC has a higher areal ratio compared to DPPC. Lipids with higher A_{hg}/A_{ch} values are expected to have less room to accommodate peptides in the headgroup region without distortion, and thus would exhibit lower threshold P/L* ratios. This explains why, for example, alamethicin inserts to a DMPC bilayer at a lower P/L* ratio as compared to a DOPC bilayer (7,45). The results obtained here for alamethicin inserted into DHPC and DPPC bilayers do not follow this rule.

Based on the OCD results, membrane thinning would therefore occur at different P/L ratios for alamethicin in DPPC versus DHPC, as a result of hydrophobic mismatch. The free energy cost of such thinning, which causes headgroup deformation, increases quadratically with the P/L. At some critical P/L*, the energy cost of thinning exceeds the energy for insertion, and the inserted state becomes favored at higher P/L ratio (5,10,16,46). Studies of lipid motility by fluorescence anisotropy report a marked instability or ''wobbling'' of lipid hydrocarbon chains as the P/L approaches P/L*, indicating that both headgroups and hydrocarbon tails are distorted as a result of membrane thinning (14). Our results from ^{31}P aligned spectra support this increase in deformation of the headgroup with increasing alamethicin concentration (vide infra).

To further characterize the insertion of alamethicin in DHPC, solid-state ^{31}P NMR spectroscopy (47) on MLV and aligned samples of alamethicin/DHPC was performed. ^{31}P static spectra of MLV samples of DHPC were recorded as a function of increasing alamethicin concentration and temperature (data not shown). The width of the powder pattern for pure DHPC was found to be 52 ppm, in agreement with the width of 55 ppm for a DHPC bilayer at 21°C (17). Experiments performed at 50°C, for which DHPC is in liquid crystalline phase, showed a reduced powder pattern width of 42 ppm. This and the fact that the axially symmetric spectral shape and CSA parameters agree well with previous ^{31}P NMR studies (17) serve to confirm that the lipid bilayers studied here are in the interdigitated-gel phase ($L_\beta I$). Addition of alamethicin to DHPC (P/L ratios = 1:80 and 1:15) does not change the spectral line shape and CSA parameters of the ^{31}P NMR spectra in any way. This indicates that the addition of alamethicin to DHPC does not lead to the formation of new phases, a result which is further confirmed by our DSC results (vide infra).

Fig. 3 *A* shows a proton-decoupled ^{31}P NMR spectra of fully hydrated MLVs of pure DHPC bilayers at 25°C. In Fig. 3 *B*, the ^{31}P NMR spectra of a mechanically aligned DHPC (pure) bilayer at 25°C is illustrated. The presence of a single intense peak at 35 ppm indicates that the DHPC bilayer normal is aligned parallel to the external magnetic field. Fig. 3, *C–G*, shows the ^{31}P NMR spectra of mechanically aligned DHPC bilayer with increasing alamethicin concentration: the P/L ratio varies from 1:90, 1:80, 1:50, and 1:30 to 1:15, respectively. The presence of an intense peak at 34 ppm indicates that a significant proportion of the DHPC membrane bilayer remains aligned even at higher peptide concentration. Comparison of Fig. 3, *E–G* with Fig. 3 *B* clearly suggests that the addition of alamethicin does, however, partially disrupt the lipid orientation, as manifested by the increased intensity at −17 ppm. This peak position represents a bilayer normal alignment perpendicular to the magnetic field. At the highest alamethicin concentration (P/L ratio = 1:15), for which alamethicin is in the *I* state (from OCD data), an additional isotropic peak appears (at ~0 ppm, Fig. 3 *G*), which could originate from either the formation of smaller vesicles/micelles, the formation of a different phase (e.g., cubic phase), or from toroidal pore defects within the bilayer (30,48).

The presence of these additional peaks (i.e., at ~−16 ppm and at the isotropic peak position) with increasing peptide concentration have also been observed in a number of other

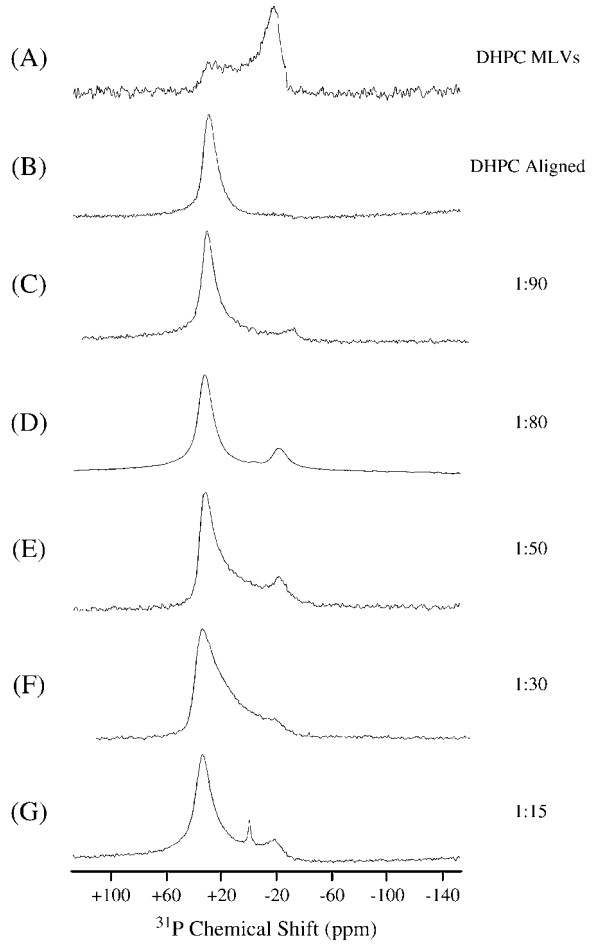

FIGURE 3 ^{31}P NMR spectra of (*A*) pure DHPC MLVs (fully hydrated); (*B*) oriented pure DHPC; and (*C–F*) oriented DHPC lipid bilayers with increasing alamethicin concentration, i.e., P/L = 1:90, 1:80, 1:50, 1:30, and 1:15, respectively. For all oriented samples, the glass plates are oriented such that the bilayer normal is oriented parallel to the magnetic field. The temperature was set at 25°C.

^{31}P NMR spectra of mechanically aligned bilayers of peptides incorporated into a range of lipid types. Examples include the peptide paradaxin incorporated into the DMPC or POPE lipid bilayers (29), myelin basic protein, inserted in the POPC lipid bilayers (49), RTD-1 incorporated into POPC, DMPC, DLPC bilayers (50), protegrin-1 (PG-1) incorporated to POPC/cholesterol bilayers (30), $K_2(LA)_xK_2$ incorporated into mechanically aligned DCPC, DLPC, DOPC, and POPC bilayers (51), LL37, an amphipathic, antimicrobial peptide which inserts into POPC/POPG, POPC/cholesterol, and POPE/POPG bilayers (52), and finally MSI-78, which forms toroidal pores in POPC at concentrations of 1–5 mol % (53). In some cases, the presence of these additional peaks and/or broadening of the peak shapes have been attributed to a peptide-induced lipid phase transition. In other cases, it has been attributed to a peptide-induced disordering effect of the peptide on the lipid bilayer, which may arise due to hydrophobic mismatch between the peptide and the lipid (51). Although, as mentioned above, the ^{31}P spectra obtained for MLV samples of DHPC/alamethicin suggest that there is no formation of a new lipid phase, we also conducted DSC experiments to determine whether alamethicin induces new phase transitions in DHPC.

Fig. 4 shows a series of DSC heating thermograms of large MLVs composed of fully hydrated DHPC, 1:80 alamethicin/DHPC, and 1:15 alamethicin/DHPC, respectively. DHPC typically undergoes two endothermic transitions upon heating: a pretransition at T_m = 34°C–35°C and a large-enthalpy main transition to liquid-crystalline phase at T_m = 44°C–45°C (43). This DSC study clearly reveals that the addition of increasing amounts of alamethicin to DHPC does not induce new phase transitions. It does, however, have a small effect, by shifting the pretransition slightly and broadening the main transition. This is consistent with previously reported data for alamethicin (37). This effect is small as compared to alamethicin in DPPC, where the thermograms reveal a phase transition temperature which is reduced slightly and a phase transition peak which is broadened extensively upon addition of alamethicin (data not shown). This is again consistent with earlier results obtained from differential thermoanalysis of DPPC in the presence of alamethicin (37).

The evidence described thus far, therefore, suggests that alamethicin induces a disordering effect on DHPC, which is a result of membrane-thinning which occurs at high alamethicin concentrations. To further quantify this disordering effect, we have performed ^{31}P inversion recovery experiments for three samples—DHPC (100%), alamethicin/DHPC (P/L = 1:80), and alamethicin/DHPC (P/L = 1:15)—to understand the headgroup motions in MLVs. To first approximation, the inversion recovery of the whole powder pattern could be described by a single $T1$ value, therefore the $T1$ relaxation values were evaluated at the −15 ppm for MLV samples (Table 1), as described in the Materials and

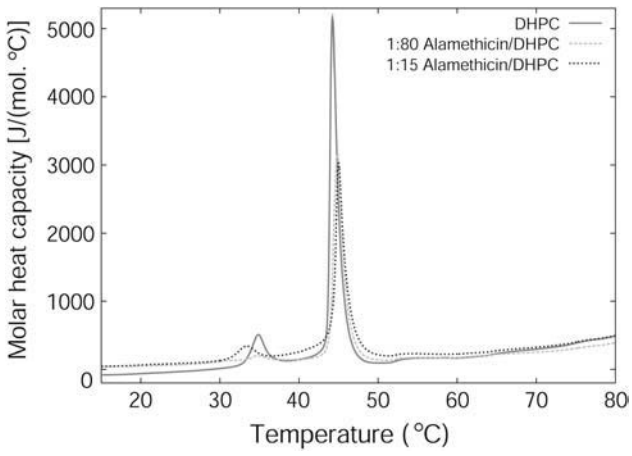

FIGURE 4 DSC heating thermograms for (*solid line*) pure DHPC, (*dashed line*) P/L = 1:80 alamethicin/DHPC, and, finally, (*dotted line*) P/L = 1:15 alamethicin/DHPC. See text for more details.

TABLE 1 *T*1 relaxation values evaluated from the ^{31}P NMR inversion recovery experiments of DHPC with varying amounts of alamethicin as a function of temperature

Sample type	Alamethicin/ DHPC P/L ratio	*T*1 at $T = 24°C$ (in ms)	*T*1 at $T = 50°C$ (in ms)
Multilamellar vesicles	DHPC (100%)	590 ± 55	473 ± 45
	1:80	505 ± 45	475 ± 55
	1:15	555 ± 55	510 ± 55

Methods section. As a check, a *T*1 value was also determined for pure POPC multilamellar vesicles ($T1 = 980 \pm 50$ ms at 24°C), which agrees with the value reported in the literature (39). For DHPC, the addition of alamethicin clearly only has a slight effect on the relaxation rate $1/T1$, with the largest effect being observed for the 1:80 alamethicin/DHPC ratio, where *T*1 is reduced by ~100 ms at 24°C. It is consistent with the model that alamethicin interacts with a larger number of DHPC headgroups when it is in a surface associated or *S* state, though the large experimental error does not prove this conclusively. The decrease in *T*1 values with increased temperature indicates that the headgroups undergo more motion in the interdigitated-gel phase than in the liquid crystalline phase at 50°C.

To try to determine whether the disordering effect of alamethicin on the DHPC bilayer is due to hydrophobic mismatch, ^{31}P NMR spectra were also measured for mechanically aligned ester-linked POPC bilayers, with the same P/L ratios. As mentioned previously, the hydrophobic length of alamethicin is 22 Å, whereas the hydrocarbon distance is 13 Å for DHPC bilayers, 24 Å for DPPC bilayers (44), and 26–27 Å for POPC bilayers (51). Consequently, one expects a proportionately larger/wider peak at −16 ppm in the ^{31}P NMR spectrum of alamethicin in aligned DHPC than in POPC. Fig. 5 *A* shows the ^{31}P NMR spectra of POPC fully hydrated MLVs at 25°C. The width of the powder pattern for pure POPC bilayers is 45 ppm, in agreement with the literature (17,46). The spectral line shape and width (Figs. 3 *A* and 5 *A*) indicate that the DHPC liposomes are in interdigitated gel phase, whereas POPC liposomes are in liquid-crystalline phase (17,46). Our results are also in agreement with the spectral line shape changes observed previously for mechanically aligned DMPC membrane bilayers from gel to intermediate and finally to liquid crystalline phase (54). Fig. 5, *B* and *C*, illustrates the ^{31}P NMR spectra of the mechanically aligned POPC bilayer with two different ratios of alamethicin to lipid: P/L = 1:80 and 1:15, respectively. The intense narrow peak at 30 ppm indicates that the bilayer normal aligns parallel to the magnetic field in the presence of alamethicin. A peak is also present at −15 ppm, suggesting that a slight disordering in the lipid headgroup region occurs. Comparison of Figs. 3 *D* with 5 *B* and Figs. 3 *F* with 5 *C* indicates that the orientation disorder of lipid headgroup is less significant in the case when alamethicin is inserted in the POPC as compared to DHPC. Therefore, the disordering effect of the peptaibol is less significant in the case of POPC as compared to DHPC, indicating that hydrophobic thickness plays a critical role in the insertion mechanism of alamethicin in the different lipids.

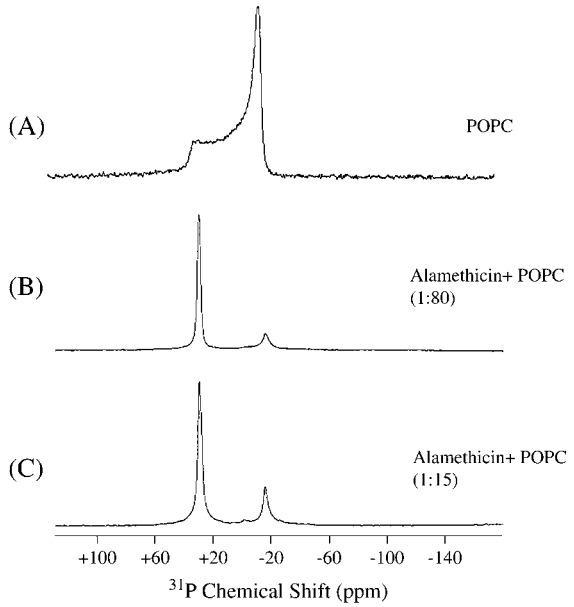

FIGURE 5 ^{31}P NMR spectra of (*A*) pure POPC MLVs (fully hydrated); (*B–C*) oriented POPC lipid bilayers with increasing alamethicin concentration, i.e., P/L = 1:80 and 1:15, respectively. For all oriented samples, the glass plates are oriented such that the bilayer normal is oriented parallel to the magnetic field. The temperature was set at 25°C.

Based on the data reported here and comparing with models for the insertion of alamethicin into ester-linked lipid bilayers (10,55–59), we therefore suggest that alamethicin inserts into DHPC bilayers, as illustrated in Fig. 6. In Fig. 6

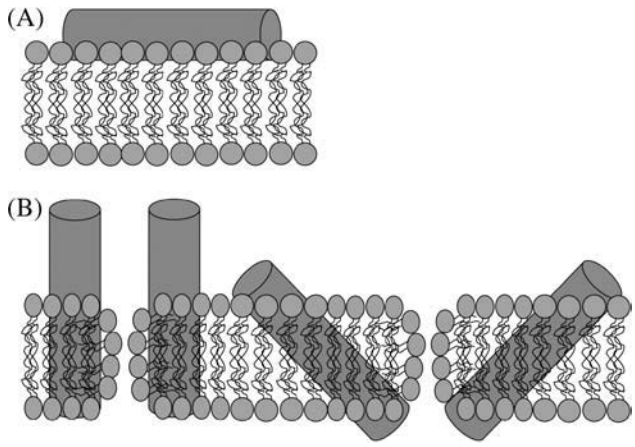

FIGURE 6 Models of alamethicin insertion, based on the data reported in this work. Alamethicin is depicted as a cylinder. (*A*) Alamethicin in ether-linked DHPC bilayer (in interdigitated-gel phase at room temperature) in the *S* state, at lower P/L ratio, whereas in *B* it is in the *I* state, at higher P/L ratios. The orientation of alamethicin is unknown at this point; therefore the peptide is shown as either partially inserting into the bilayer (*left*) or inserting/tilting into the bilayer (*right*) to accommodate the large hydrophobic mismatch.

A, at low P/L ratios, alamethicin is oriented perpendicular to the lipid bilayer normal or surface adsorbed, with small perturbations of the lipid headgroup. With higher and higher P/L ratios, alamethicin increasingly inserts into the lipid bilayer, with increasing perturbation of some of the lipid headgroups (Fig. 6 *B*). Given the shape of the ^{31}P NMR signals observed in the aligned samples (53,60) and that the perturbation of the lipids gradually increases as more and more alamethicin inserts into the membrane (i.e., given that the peptide is always associated with the lipid headgroup (10)), we propose that alamethicin inserts into DHPC using a toroidal mechanism. Indeed the peak shapes observed at P/L ratios in the range 1:50–1:15 are practically identical to the simulated ^{31}P NMR lineshapes presented in Hallock et al. (53). Moreover, since DHPC has a headgroup area which is larger than the alkyl chain, it can easily accommodate the positive curvature required for the toroidal model. This mechanism for alamethicin insertion is different from that for POPC bilayers, which is the barrel-stave mechanism (10,55–59). One should note that to prove our toroidal model conclusively, single channel conductance measurements would be needed (55). Finally, it should be emphasized that the arrangement of alamethicin in DHPC bilayers is at this point undetermined. The peptide may insert partially or it could oligomerize or tilt (61) to minimize the large hydrophobic mismatch between alamethicin and DHPC in the interdigitated phase. ^{15}N (or ^{13}C) NMR measurements would be needed to further determine the orientation of alamethicin in DHPC (28).

CONCLUSIONS

In this study, we have shown that alamethicin inserts into both ether-linked DHPC bilayers and ester-linked DPPC or POPC bilayers. The OCD results show that at a lower P/L ratio, alamethicin lies on the surface of the ether-linked DHPC membrane, whereas it inserts into the bilayer at a higher P/L ratio. The P/L* threshold is higher for alamethicin in DHPC (between 1:40 and 1:30) than in DPPC (~1:80) at 20°C. This is likely due to the relative differences in the hydrophobic length of alamethicin, DHPC, and DPPC. The ^{31}P NMR data show how alamethicin increasingly perturbs the DHPC headgroup with increasing alamethicin concentration, finally leading to additional peaks at −16 ppm and at the isotropic position. This is not accompanied by a change in phase of the lipids, as confirmed by the DSC data. Given the results, we therefore propose that alamethicin inserts into DHPC bilayers using the toroidal model. Further studies on the orientation of alamethicin in DHPC are currently underway.

The authors thank David Jung (in Prof. Robert E. W. Hancock's laboratory, Dept. of Microbiology and Immunology, University of British Columbia (UBC)) for help with the DSC measurements. The measurements were performed at the UBC Centre for Biological Calorimetry. The authors also thank Dr. Fred Rosell of the UBC Laboratory of Molecular Biophysics Spectroscopy and Kinetics Hub for useful discussions about the OCD experiments.

S.K.S. acknowledges financial support from the Natural Sciences and Engineering Research Council of Canada (Discovery Grant and University Faculty Award) and UBC.

This work was presented in part at the 46th Experimental NMR Conference (ENC), Providence, RI, April 11–15, 2005.

REFERENCES

1. Jen, W. C., G. A. Jones, D. Brewer, V. O. Parkinson, and A. Taylor. 1987. The antibacterial activity of alamethicin and zervamicins. *J. Appl. Bacteriol.* 63:293–298.
2. Bechinger, B. 1997. Structure and functions of channel-forming peptides: maganins, cecropins, melittin and alamethicin. *J. Membr. Biol.* 156:197–211.
3. Bechinger, B. 2000. Solid-state NMR investigations on the structure and topological equilibria of polypeptides associated with biological membranes. *Phys. Chem. Chem. Phys.* 2:4569–4573.
4. He, K., S. J. Ludtke, and H. W. Huang. 1995. Antimicrobial peptide pores in membranes detected by neutron in-plane scattering. *Biochemistry.* 34:15614–15618.
5. He, K., S. J. Ludtke, D. L. Worcester, and H. W. Huang. 1996. Neutron scattering in the plane of membranes: structure of alamethicin pores. *Biophys. J.* 70:2659–2666.
6. Chen, F., M. Lee, and H. W. Huang. 2002. Sigmoidal concentration dependence of antimicrobial peptide activities: a case study on alamethicin. *Biophys. J.* 82:908–914.
7. Huang, H. W., and Y. Wu. 1991. Lipid-alamethicin interactions influence alamethicin orientation. *Biophys. J.* 60:1079–1087.
8. Banerjee, U., R. Zidovetski, R. R. Birge, and S. I. Chan. 1985. Interaction of alamethicin with lethicin bilayers: A ^{31}P and ^{2}H NMR study. *Biochemistry.* 40:9428–94377.
9. Yang, L., T. A. Harroun, T. M. Weiss, L. Ding, and H. W. Huang. 2001. Barrel-stave model or toroidal model? A case study on melittin pores. *Biophys. J.* 81:1475–1485.
10. Bak, M., R. P. Bywateer, M. Hohwy, J. K. Thomsen, K. Adelhorst, H. J. Jakobsen, O. W. Sorensen, and N. C. Nielsen. 2001. Conformation of alamethicin in oriented phospholipid bilayers determined by N-15 solid-state nuclear magnetic resonance. *Biophys. J.* 81:1684–1698.
11. Ludtke, S. J., K. He, Y. Wu, and H. W. Huang. 1994. Cooperative membrane insertion of magainin correlated with its cytolytic activity. *Biochim. Biophys. Acta.* 1190:182–184.
12. Ludtke, S. J., K. He, and H. W. Huang. 1994. Membrane thinning caused by maganin 2. *Biochemistry.* 34:16764–16769.
13. Heller, W. T., A. J. Waring, R. I. Lehrer, and H. W. Huang. 1998. Multiple states of beta-sheet peptide protegrin in lipid bilayers. *Biochemistry.* 37:17331–17338.
14. Kikukawa, T., and T. Araiso. 2002. Changes in lipid mobility associated with alamethicin incorporation into membranes. *Arch. Biochem. Biophys.* 405:214–222.
15. Heller, W. T., K. He, S. J. Ludtke, T. A. Harroun, and H. W. Huang. 1997. Effect of changing the size of lipid headgroup on peptide insertion into membranes. *Biophys. J.* 73:239–244.
16. Wu, Y., K. He, S. J. Ludtke, and H. W. Huang. 1995. X-ray diffraction study of lipid bilayer membranes interacting with amphiphilic helical peptides: diphytanoyl phosphatidylcholine with alamethicin at low concentrations. *Biophys. J.* 68:2361–2369.

17. Ruocco, M. J., D. J. Siminovitch, and R. G. Griffin. 1985. Comparative study of the gel phases of ether- and ester-linked phosphatidylcholines. *Biochemistry.* 24:2406–2411.

18. Laggner, P., K. Lohner, G. Degovics, K. Muller, and A. Schuster. 1987. Structure and thermodynamics of the dihexadecylphosphatidylcholine-water system. *Chem. Phys. Lipids.* 44:31–60.

19. Kim, J. T., J. Mattay, and G. G. Shipley. 1987. Gel phase polymorphism in ether-linked dihexadecylphosphatidylcholine bilayers. *Biochemistry.* 26:6592–6598.

20. Lohmeyer, M., and R. Bittman. 1994. Antitumor ether lipids and alkylphosphocholines. *Drugs Future.* 19:1021–1037.

21. Bloom, M., and O. G. Mouritsen. 1995. The evolution of membrane structure and dynamics of membrane. *In* Handbook of Biological Physics, Vol. 1A. R. Lipiwsky and E. Sackman, editors. Elsevier/North Holland, Amsterdam. 65–95.

22. Yang, J., P. D. Parkanzky, M. L. Bodner, C. A. Duskin, and D. P. Weliky. 2002. Application of REDOR subtraction for filtered MAS observation of labeled backbone carbons of membrane-bound fusion peptides. *J. Magn. Reson.* 159:101–110.

23. Bodner, M. L., C. M. Garbys, P. D. Parkanzky, J. Yang, C. A. Duskin, and D. P. Weliky. 2004. Temperature dependence and resonance assignment of ^{13}C NMR spectra of selectively and uniformly labeled fusion peptides associated with membranes. *Magn. Reson. Chem.* 42:187–194.

24. Cavagnero, S., H. J. Dyson, and P. E. Wright. 1999. Improved low pH bicelle system for orienting macromolecules over a wide temperature range. *J. Biomol. NMR.* 13:387–391.

25. Ottiger, M., and A. Bax. 1999. Bicelle-based liquid crystals for NMR measurement of dipolar couplings at acidic and basic pH values. *J. Biomol. NMR.* 13:187–191.

26. De Angelis, A. A., A. A. Nevzorov, S. H. Park, S. C. Howell, A. A. Merse, and S. J. Opella. 2004. High-resolution NMR spectroscopy of membrane proteins in aligned bicelles. *J. Am. Chem. Soc.* 126: 15340–15341.

27. Chen, F., M. Lee, and H. W. Huang. 2002. Sigmoidal concentration dependence of antimicrobial peptide activities: a case study on alamethicin. *Biophys. J.* 82:908–914.

28. Bechinger, B., D. A. Skladnev, A. Ogrel, X. Li, E. V. Rogozhkina, T. Ovchinnikova, V. O'Neil, and J. D. J. Raap. 2001. ^{15}N and ^{31}P solid-state NMR investigations on the orientation of Zervamicin II and alamethicin in phosphatidylcholine membranes. *Biochemistry.* 40: 9428–9437.

29. Hallock, K. J., D. K. Lee, J. Omnaas, H. I. Mosberg, and A. Ramamoorthy. 2002. Membrane composition determines pardaxin's mechanism of lipid bilayer disruption. *Biophys. J.* 83: 1004–1013.

30. Mani, R., J. J. Buffy, A. J. Waring, R. I. Lehrer, and M. Hong. 2004. Solid-state NMR investigation of the selective disruption of lipid membranes by protegrin-1. *Biochemistry.* 43:13839–13848.

31. Lohner, K., E. Staudegger, E. J. Penner, R. N. A. H. Lewis, M. Kriechbaum, G. Dagovics, and R. N. McElhaney. 1999. Effect of staphylococcal δ-lysin on the thermotropic phase behavior and vesicle morphology of dimyristoylphosphatidulcholine lipid bilayer model membranes. Differential scanning calorimetric, ^{31}P nuclear magnetic resonance and Fourier transform infrared spectroscopic, and x-ray diffraction studies. *Biochemistry.* 38:16514–16528.

32. Cullis, P. R., and B. De Kruyff. 1976. ^{31}P NMR studies of unsonicated aqueous dispersions of neutral and acidic phospholipids. Effects of phase transitions, p2H and divalent cations on the motion in the phosphate region of the polar headgroup. *Biochim. Biophys. Acta.* 436:523–540.

33. Huang, C., and S. Li. 1999. Calorimetric and molecular mechanics studies of the thermotropic phase behavior of membrane phospholipids. *Biochim. Biophys. Acta.* 1422:273–307.

34. Epand, R. M., and W. K. Surewicz. 1984. Effect of phase transitions on the interaction of peptides and proteins with phospholipids. *Can. J. Biochem. Cell Biol.* 62:1167–1173.

35. Prenner, E. J., R. N. Lewis, K. C. Neuman, S. M. Gruner, L. H. Kondejewski, R. S. Hodges, and R. N. McElhaney. 1997. Nonlamellar phases induced by the interaction of gramicidin S with lipid bilayers. A possible relationship to membrane-disrupting activity. *Biochemistry.* 36:7906–7916.

36. Henzer-Wildman, K. A., G. V. Martinez, M. F. Brown, and A. Ramamoorthy. 2004. Perturbation of the hydrophobic core of lipid bilayers by the human antimicrobial peptide LL-37. *Biochemistry.* 43:8459–8469.

37. Freisleben, H. J., D. Blocher, and K. Ring. 1992. Calorimetry of tetraether lipids from Thermoplasma acidophilum: incorporation of alamethicin, melittin, valinomycin, and nonactin. *Arch. Biochem. Biophys.* 294:418–426.

38. de Jongh, H. H., E. Goormaghtigh, and J. A. Killian. 1994. Analysis of circular dichroism spectra of oriented protein-lipid complexes: toward a general application. *Biochemistry.* 33:14521–14528.

39. Tamm, L. K., and J. Seelig. 1983. Lipid solvation of cytochrome c oxidase. Deuterium, nitrogen-14, and phosphorus-31 nuclear magnetic resonance studies on the phosphocholine head group and on cis-unsaturated fatty acyl chains. *Biochemistry.* 22:1474–1483.

40. Pinheiro, T. J. T., and A. Watts. 1994. Lipid specificity in the interaction of cytochrome-c with anionic phospholipids-bilayers revealed by solid-state P-31 NMR. *Biochemistry.* 33:2451–2458.

41. Pinheiro, T. J. T., and A. Watts. 1994. Resolution of individual lipids in mixed phospholipids membranes and specific lipid-cytochrome c interactions by magic-angle spinning solid-state phosphorus-31 NMR. *Biochemistry.* 33:2459–2467.

42. Wu, Y., H. W. Huang, and G. A. Olah. 1990. Method of oriented circular dichroism. *Biophys. J.* 57:797–806.

43. Hing, F. S., and G. G. Shipley. 1995. Molecular interactions of ether-linked phospholipids. *Biochemistry.* 34:11904–11909.

44. Hirsh, D. J., N. Lazaro, L. R. Wright, J. M. Boggs, T. J. McIntosh, J. Schaefer, and J. Blazyk. 1998. A new monofluorinated phosphatidylcholine forms interdigitated bilayers. *Biophys. J.* 75:1858–1868.

45. Hung, W. C., F. Y. Chen, and H. W. Huang. 2000. Order-disorder transition in bilayers of diphytanoyl-phosphatidylcholine. *Biochim. Biophys. Acta.* 1467:198–206.

46. Heller, W. T., A. J. Waring, R. I. Lehrer, T. A. Harroun, T. M. Weiss, L. Yang, and H. W. Huang. 2000. Membrane thinning effect of the beta-sheet antimicrobial protegrin. *Biochemistry.* 39:139–145.

47. Seelig, J. 1978. P-31 nuclear magnetic-resonance and head group structure of phospholipids in membrane. *Biochim. Biophys. Acta.* 515:105–140.

48. Prenner, E. J., R. N. Lewis, and R. N. McElhaney. 1999. The interaction of the antimicrobial peptide gramicidin S with lipid bilayer model and biological membranes. *Biochim. Biophys. Acta.* 1462: 201–221.

49. Pointer-Keenan, C. D., D. K. Lee, K. Hallock, A. M. Tan, R. Zand, and A. Ramamoorthy. 2004. Investigation of the interaction of myelin basic protein with phospholipid bilayers using solid-state NMR spectroscopy. *Chem. Phys. Lipids.* 132:47–54.

50. Buffy, J. J., M. J. McCormick, S. Wi, A. Waring, R. I. Mehrer, and M. Hong. 2004. Solid-state NMR investigation of the selective perturbation of lipid bilayers by the cyclic antimicrobial peptide RTD-1. *Biochemistry.* 43:9800–9812.

51. Harzer, U., and B. Bechinger. 2000. Alignment of lysine-anchored membrane peptides under conditions of hydrophobic mismatch: A CD, ^{15}N and ^{31}P solid-state NMR spectroscopy investigation. *Biochemistry.* 39:13106–13114.

52. Henzer-Wildman, K. A., D. K. Lee, and A. Ramamoorthy. 2003. Mechanism of lipid bilayer disruption by the human antimicrobial peptide, LL-37. *Biochemistry.* 42:6545–6558.

53. Hallock, K. J., D. K. Lee, and A. Ramamoorthy. 2003. MSI-78, an analogue of the magainin antimicrobial peptides, disrupts lipid bilayer structure via positive curvature strain. *Biophys. J.* 84:3052–3060.

54. Dufourc, E. J., C. Mayer, J. Stoher, G. Althoff, and G. Kothe. 1992. Dynamics of phosphate head groups in biomembranes. *Biophys. J.* 61:42–57.

55. Mak, D. O., and W. W. Webb. 1995. Two classes of alamethicin transmembrane channels: molecular models from single-channel properties. *Biophys. J.* 69:2323–2336.

56. North, C. L., M. Barranger-Mathys, and D. S. Cafiso. 1995. Membrane orientation of the N-terminal segment of alamethicin determined by solid-state N-15 NMR. *Biophys. J.* 69:2392–2397.

57. Sansom, M. S. 1993. Alamethicin and related peptaibols-model ion channels. *Eur. Biophys. J.* 22:105–124.

58. Tieleman, D. P., M. S. P. Sansom, and H. J. C. Berendsen. 1999. Alamethicin helices in a bilayer and in solution: molecular dynamics simulations. *Biophys. J.* 76:40–49.

59. Tieleman, D. P., H. J. C. Berendsen, and M. S. P. Sansom. 1999. An alamethicin channel in a lipid bilayer: molecular dynamics simulations. *Biophys. J.* 76:1757–1769.

60. Thennarasu, S., D. K. Lee, A. Tan, U. Prasad Kari, and A. Ramamoorthy. 2005. Antimicrobial activity and membrane selective interactions of a synthetic lipopeptide MSI-843. *Biochim. Biophys. Acta.* 1711:49–58.

61. Killian, J. A. 1998. Hydrophobic mismatch between proteins and lipids in membranes. *Biochim. Biophys. Acta.* 1376:401–416.